The universe is static

David F. Crawford[1]

44 Market St, Naremburn, 2065, NSW, Australia

Abstract

It is shown that the light curve widths of type Ia supernovae do not have time dilation and that their magnitudes are consistent with a static universe. The standard analysis for type Ia supernovae uses a set of templates to overcome the intrinsic variation of the supernova light curves with wavelength. The reference light curves derived from this set of templates contain an anomaly in that at short wavelengths the width of the light curve is proportional to the emitted wavelength. Furthermore this anomaly is exactly what would be produced if supernovae at different redshifts did not have time dilation and yet time dilation corrections were applied. It is the specific nature of this anomaly that is evidence for a static universe. The lack of time dilation is confirmed by direct analysis of the original observations. It is also found that the peak flux density of the light curves in the reference templates had a strong dependence on wavelength that could be due to the use of an incorrect distance modulus. This dependence is investigated by computing the peak absolute magnitudes of type Ia supernovae observations from the original observations using a static cosmological model. The results support the hypothesis of a static universe. It is also argued that the photometric redshift relation and spectroscopic ages are consistent with a static universe.

Keywords: cosmology:miscellaneous, supernovae:general

1. Introduction

Type Ia supernovae are transient phenomena that take about ten days to reach a peak brightness and then the brightness decreases at a slower rate. Type Ia supernovae (for brevity SNe) are also known for their remarkably constant absolute peak magnitudes and this property makes them excellent cosmological probes. For example the width of the light curves is one of the few cosmological observations that can directly measure time dilation at large redshifts.

The observed Hubble redshift, z, is defined as the ratio of the observed wavelength to the emitted wavelength minus one. In an expansion model the ratio of any observed time period to the emitted time period is identical to the ratio of the wavelengths, namely $(1 + z)$. This is true for any time interval and is the time dilation that is applicable to the widths of the supernova light curves. Any challenge to the standard model, such as a static model, must show that observations of SNe light-curve widths do not have time dilation even though the observed spectral lines show a redshift.

The first strong evidence for time dilation in type Ia supernovae was provided by Leibundgut et al. [26] with one supernova and Goldhaber et al. [17] with seven SNe. This was quickly followed by multiple SNe results from Goldhaber [16], Perlmutter et al. [28], Goldhaber et al. [18]. These papers record developments in both SNe observations and analysis, the results of which are asserted to provide strong evidence for an expansion model chiefly because they show that the width of type Ia supernova light curves appears to increase with redshift in good agreement with an expanding model.

The results of this paper are based on the extensive analysis of type Ia supernova observations provided by Betoule et al. [3] (hereafter B14).

This paper has two major sections. The first one (section 6) argues that the width of the light curve does not show any time dilation. The second section (section 7 shows that the peak luminosity is consistent with as static universe. Since these properties of the light curve are orthogonal there is no direct observational relationship between them.

There is an intrinsic variation of the shape of light curves of SNe with emitted wavelength, which needs to be removed in order to measure the peak luminosity and width for each supernova. This removal is done by comparing the observations of each supernova to a reference light curve obtained for each filter from a set of templates.

However the set of templates used by B14 contains an anomaly in that the width of the reference light curve derived from these templates at short wavelengths is proportional to the rest-frame wavelength. It is argued that this relationship is an anomaly because it is completely unexpected in the standard cosmological model. Importantly, this anomaly is exactly what would be produced if the epoch differences were not subject to time dilation and yet time dilation corrections are applied. It is the specific nature of this anomaly that is evidence for a static universe.

A re-analysis of the original SNe observations without using the B14 templates shows that the widths of the SNe light curves are fully consistent with having no time dilation. Note that this analysis and its conclusion are independent of any cos-

---

mological model and only depend on the presence or absence of time dilation. The implication is that the universe is static.

In section 7 it is shown that the peak flux density of the reference light curves that are used to remove the intrinsic dependent of luminosity on emitted wavelength shows a very strong dependence on wavelength that could be due to the use of an incorrect distance modulus.

This dependence is investigated by plotting the peak absolute magnitudes for each supernova as a function of redshift. These magnitudes are derived from the original observations and do not use the B14 calibration method. If the correct distance modulus is used the absolute magnitudes should scatter about a constant value. After corrections for the average peak magnitudes the absolute peak magnitudes derived using the static model have a very small dependence on redshift whereas those derived using an expansion model have a large and very significant dependence on redshift.

There are two further findings from SNe observations that appear to support the expansion model. First is the apparent dependence of photometric-redshift observations on redshift. These are observations that photometric properties of type Ia supernova spectra, as distinct from spectral wavelength measurements used to determine redshift, show a redshift dependence. However what they show is a light-curve width dependence not a redshift dependence. Second the age of a spectrum is the number of days between the observation of the spectrum and the epoch of the peak magnitude of the supernova. The ability to determine the age from subtle changes in the spectrum provides an independent method of estimating the light-curve width of the supernova. Provided it is not interpreted as a redshift dependence this light-curve width dependence is consistent with a static cosmology.

The distance modulus (equation A.5) for the static model are described in Appendix A. The expansion model distance-modulus used is for the modified Λ-CDM model (the required equations are provided in Appendix B). For both cosmologies the reduced Hubble constant is h=0.7.

2. The supernovae data set

Recently B14 have provided an update of the Conley et al. [5] analysis with better optical calibrations and more SNe. This JLA (Joint Light-curve Analysis) list sample has 720 SNe from the Supernova Legacy Survey (SNLS), nearby SNe (LowZ), the Sloan Digital Sky Survey (SDSS) [23, 25] and those revealed by the Hubble Sky Telescope (HST) [30]. The B14 data file provided the supernova name, the redshift, the apparent magnitude and its uncertainty, the stretch parameter (x_1) and its uncertainty, the color parameter (C) and its uncertainty, the host stellar mass and finally the survey number. The stretch factor was calculated using the equation [21]

$$s_{B14} = 0.98 + 0.091x_1 + 0.003x_1^2 - 0.00075x_1^3 \quad (1)$$

The B14 calibration method [? 21] uses the SALT2 templates (Spectral Adaptive Light-curve Templates) which provide the expected flux density of the supernova light curve as

a function of the rest-frame wavelength and the difference between the observed epoch and the epoch of maximum response. The standard Salt2 template file, $Salt2\_template\_0.dat$, provides the response for approximately 20 days prior to the maximum and 50 days after the maximum for rest-frame wavelengths from 200 nm to 920 nm in steps of 0.5 nm. The template file for the JLA analysis was taken from the SNANA [25] website in the directory $models/SALT2/SALT2.JLA-B14$.

3. The B14 calibration method

The B14 calibration method uses the set of SALT2 [? 21] templates described in section 2. The major purpose of the method is to remove intrinsic variations of the shape of light curves of SNe with emitted wavelength. This removal is done by comparing the observations of each supernova to a reference light curve obtained for each filter from a set of templates. By assuming that the SNe are identical at all redshifts the beauty of the SALT2 method is that it uses the average of the light curves from all the observed SNe in order to compute the set of templates. It should be noted that the Salt2 templates are the result of a complex analysis that requires the de-convolution of the observed filter response, allowance for strong correlations and the fitting of auxiliary parameters.

Consider the hypothetical situation where there are a large number of SNe at the same redshift. Then the reference light curve is the average of all the light curves. The estimation of the width and peak luminosity is relative to this reference light curve and is completely independent of cosmology. The SALT2 method extends this process to all observed wavelengths by averaging the light curves as a function of rest-frame (emitted frame) wavelength. The result is a set of light curve templates that are estimates of the intrinsic SNe light curve as a function of emitted wavelength. However, as shown below, in a static universe the width of the light curve either from time dilation or from corrections for time dilation can be completely included in the reference templates. Consequently this width dependence from the calibration procedure can completely nullify the time dilation (or its correction) in a subsequent analysis. Thus the width estimates using the Salt2 templates are the same as the intrinsic widths for either an expanding or a static cosmology.

4. B14 Magnitudes and stretch factors

This is brief summary of some of the results provided by B14. Following B14 the corrected apparent magnitude, m, for each supernova is

$$m = m^* + \alpha x_1 - \beta C \quad (2)$$

where m^* is the observed B band apparent peak-magnitude, x_1 the is light-curve stretch parameter and C is the color-measure. The constant α is the coefficient for the Phillips relation and β is the coefficient for the color index. The values were taken from B14 Table 14 and are $\alpha = 0.141$ and $\beta = 3.102$. The regression equations for the absolute magnitude, $M = m - \mu_{exp}$ (where μ_{exp} is the distance modulus for the expanding model,

file	counts
lcmerge/LOWZ_JRK07	48
lcmerge/JLA2014_CSP.LIST	13
lcmerge/JLA2014_CfAIII_KEPLERCAM.LIST	32
lcmerge/JLA2014_CfAIII_4SHOOTER.LIST	21
lcmerge/SNLS3year_JRK07.LIST	2
lcmerge/SDSS_allCandidates+BOSS_HEAD.FITS	369
lcmerge/JLA2014_SNLS.LIST	238
lcmerge/JLA2024_HST.LIST	9
lcmerge/SDSS_HOLTZ08	1

equation B.2) as a function the redshift is $M_{exp} = -19.095 \pm 0.006 + (0.042 \pm 0.024)z$. This shows that M_{exp} satisfies the main requirement that it is independent of redshift. However the regression for the stretch factor, $s_{B14} = 0.953 \pm 0.003 + (0.099 \pm 0.017)z$, shows a significant slope. It is this slope that has been explained by the hypothesis of dark energy.

5. The original observations

To complement the template analysis a simplified analysis of the original observations used by B14 has been done. Most of the original observations were retrieved from the SNANA [25] website using the index files shown in Table 1. The final column shows the number of B14 SNe that were recovered from each set of files. There were 7 SNe in the B14 list that could not be found in the SNANA files.

They are: sn2004s, sn1999a0, SDSS13411, SDSS15411, SDSS20088, SDSS13689, and SDSS400.

For each supernova the following data was extracted: the supernova name and for each epoch and for each filter the flux density and its uncertainty. Most of the SNe were observed in four or five filters. Following B14 the data for the filters u and U was not used.

This data was re-analyzed without using the SALT2 method. It is assumed that the central part of the light curve could be modelled by a Gaussian distribution of the flux densities as a function of the epoch differences. It is convenient to work in magnitudes where the Gaussian is equivalent to a parabola. The analysis was done separately for each filter and for each supernova. If the epoch difference is x then the expected magnitude is $a + bx + cx^2$ where a is the peak magnitude and the measured width is $w = 1/\sqrt{c}$. A weighted least squares fit was used with b being minimized in order to find the epoch of maximum flux density. One advantage of this method is that it provides estimates of the uncertainties.

In order to avoid any bias as many SNe were accepted as possible. The only selection criterion was that there had to be at least four epochs with good data within 30 days of the epoch of peak flux density and that a parabola could be fitted. The selection of the 30 day limit was a compromise between number of observations and the ability of a Gaussian to match the light curve. Individual magnitudes were omitted if during the

fit their difference from the best fit parabolic equation was more that five times the average rms for the remaining magnitudes. This was done one at a time until either there was no further omission or the number of magnitudes was less than four. Out of the 733 SNe that were found in the files 667 were accepted. For the 2398 filter sets there were 1567 that satisfied the acceptance criteria. In these filter sets there were 23700 good flux densities and 1700 flux densities that failed the individual test. Finally the supernova sn2006py appeared to have anomalous flux densities and was omitted from the analysis.

Using filter gain factors the width values from each filter were spread out over the rest-frame wavelengths and averaged over all the observations. On the assumption that the SNe are identical at all redshifts this is an estimate of the intrinsic width as a function of emitted wavelength. Similarly the apparent magnitudes were combined with a distance modulus to determine the intrinsic magnitude as a function of emitted wavelength. There are two functions one for the expanding model using equation B.2 and the other for the static model using equation A.5. This analysis mimics the principle of the Salt2 analysis but only for the two scale factors of the light curve and not for the full light curve and the auxiliary parameters.

6. Time dilation in type Ia supernovae

In the standard model used by B14 it is assumed that the time dilation is exactly compensated by the time dilation correction so that in the generation of the templates the only information that is in the templates comes from the intrinsic variations of the supernovae. Then when the templates are used to analyze a supernova the intrinsic variations in the reference light curve exactly match those in the observed supernova and the measured peak luminosity and width are relative to the average width.

Consider a static universe where the light curve widths of the SNe do not have any time dilation. Then if the time dilation correction is still applied the light curve width of a supernova at an observed wavelength λ_0 is $w = w_0/(1 + z)$ where w_0 is the reference width. The generation of the templates requires that this width is the average for the rest-frame wavelength $\lambda = \lambda_0/(1 + z)$. Hence by replacing $(1 + z)$ by the wavelength ratio the average width as a function of λ is $w = w_0\lambda/\lambda_0$ which shows that the width of the reference light curve is proportional to the rest-frame wavelength. The crucial point is that this is true for any observed wavelength and that w_0/λ_0 is a common scaling constant. Since the time dilation correction is applied to a target supernova its effect will be cancelled by the same dependence in the reference light curve. Thus the measured light curve width will be relative to the average light curve width. This explains why, if the universe is static, the time dilation correction is not seen in the B14 stretch factors. It is hidden in the set of reference templates.

The next step is to measure the light curve widths in the file $Salt2\_template\_0.dat$ and investigate their relationship to the rest-frame wavelength. The light curve width was measured from the average of three adjacent light curves at every second wavelength (i.e. at a step of 1 nm). The analysis was identical
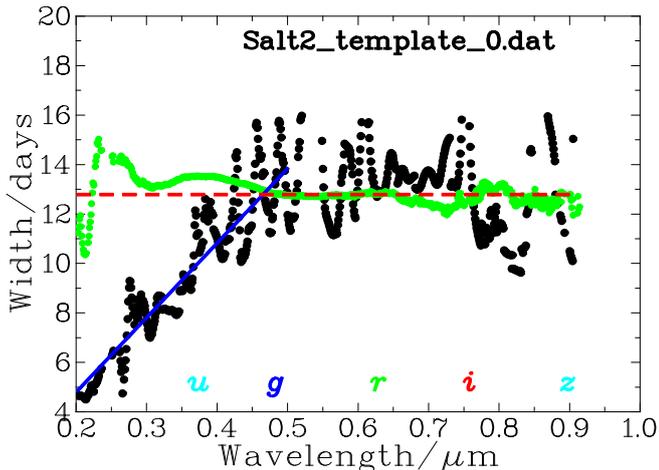
Figure 1: Plot of the relative width in days of the SALT2 template SNe light curves as a function of the relative rest-frame wavelength λ and shown as solid black circles. The blue straight line is what is expected if the light curves of the supernovae do not have time dilation. The red (horizontal) dashed line is what is expected if the light curves of the SNe have the expansion time dilation of $(1 + z)$. The green curve is the estimate of the intrinsic width from the original observations (section 5). The rest-frame wavelength for average response for each filter is shown at the bottom for the *ugriz* filters.

to parabolic procedure described in section 5. For nearby SNe the observed wavelength is almost the same as the rest-frame wavelength and therefore the templates will be poorly determined in the gaps between the filters. Consequently there were some wavelengths where the light curve did not have a strong maximum and the estimated widths were large. The results of this analysis of the B14 Salt2 templates is shown in Fig 1 as solid black circles. The green curve is the estimate of the intrinsic width from the original observations (section 5). Since these widths were relative widths for each filter the intrinsic distribution has been multiplied by 12.8 days.

If there is minimal intrinsic width variation and the time dilation is fully compensated the width should be constant for all redshifts. However in a static universe the widths should be proportional to the rest-frame wavelength. The rest-frame wavelength positions of the *ugriz* are shown in Fig 1. The reason why this proportionality is not observed at long wavelengths is that the range of the observed wavelengths covers about half of the rest-frame range. Since there are a large number of nearby SNe and all filters are given the same time dilation correction the expected distribution should be roughly constant at long wavelengths and change to being proportional to the wavelength at short wavelengths. This is exactly what is observed.

The regression equation for the Salt2 widths as a function of wavelength for the range of wavelengths between 0.2 μm and 0.53 μm is

$$w = (-1.25 \pm 0.07) + (30.15 \pm 0.77)\lambda \text{ days}. \qquad (3)$$

with a correlation coefficient of 0.918. For wavelengths longer than 0.53 μm the average value is 12.78 ± 0.09 days and is shown as a horizontal red line. This regression and the plot in Fig 1 favor a static universe that has no time dilation.

Table 2: **Asymptotic widths of original observations for all filters**

Filter	Number	mean λ/μm	w_0 /days	Slope of w/w_0
B	59	0.436	15.48 ± 0.38	2.75 ± 1.48
V	60	0.542	21.10 ± 0.52	0.30 ± 1.56
R	33	0.619	21.41 ± 0.87	-0.22 ± 0.38
I	23	0.758	24.06 ± 1.40	-0.24 ± 0.52
g	371	0.472	14.55 ± 0.21	0.27 ± 0.09
i	415	0.758	22.14 ± 0.28	0.75 ± 0.05
z	133	0.889	24.87 ± 0.77	0.45 ± 0.10

Table 2 shows the results of fitting a regression equation of the light curve widths that come from the original observations. The columns show the filter name, the number of widths, the mean wavelength, the asymptotic width at zero redshift and its uncertainty. The weighted mean redshift is 19.6 days. This table shows that each filter has a different zero value width which could be due to a different intrinsic width for its wavelength band. Consequently the widths for each filter were reduced to relative widths by dividing them by the filter zero value. (Using a common width factor made trivial differences to the final results.) The slopes of the regression of the relative widths as a function of wavelength for each filter is shown in the last column of Table 2. For an expanding model they should be about one.

Fig 2 shows a scatter diagram of the relative widths for each filter as a function of redshift and their weighted regression equation for 1617 (without HST) filter sets is shown in equation 4. These are the raw widths and they have not been corrected by a calibration template. The slope of the regression equation is statistically equivalent to zero and it is consistent with the hypothesis that there is no time dilation in type Ia supernovae.

$$w/w_0 = 1.014 \pm 0.006 + (0.020 \pm 0.024)z \qquad (4)$$

The green curve in Fig 1 shows that there is a significant variation in the intrinsic width as a function of wavelength which may explain the lack of time dilation in the SNe. Fig 3 shows a scatter diagram of the relative widths for each filter minus the intrinsic width at the average rest-frame wavelength of the filter as a function of redshift. The weighted regression equation for 1539 filter sets is shown in equation 5.

$$w/w_0 = -0.017 \pm 0.005 - (0.001 \pm 0.022)z \qquad (5)$$

As expected the scatter of the points in Fig 3 is less than the scatter in Fig 2. The important result is that the observed dependence of the widths on redshift is still insignificant which means that the effects of intrinsic width variations with wavelength cannot explain the lack of observed time dilation in the light curve widths from the original observations.

Not only does the concept of dark energy not have any meaning in a static universe but the analysis of the original observations does show any redshift dependence of light curve width on redshift.
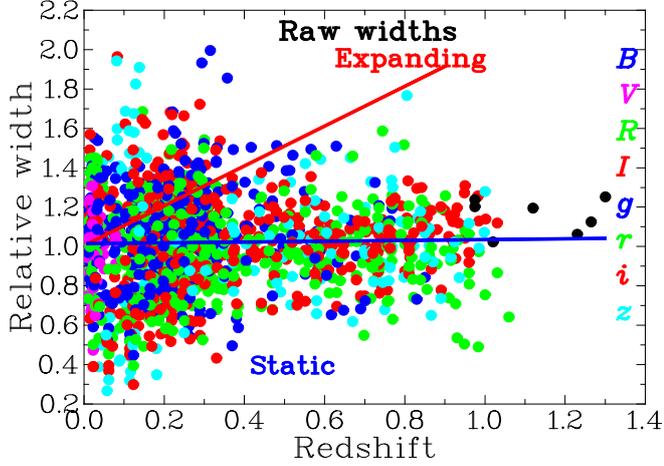
4

Figure 2: Relative light curve widths (without any corrections for time dilation) from the original observations for each filter. The blue line is the regression equation $w/w_0 = 1.014 + 0.020z$. The red line is what would be expected if the supernovae had time dilation of $(1 + z)$.
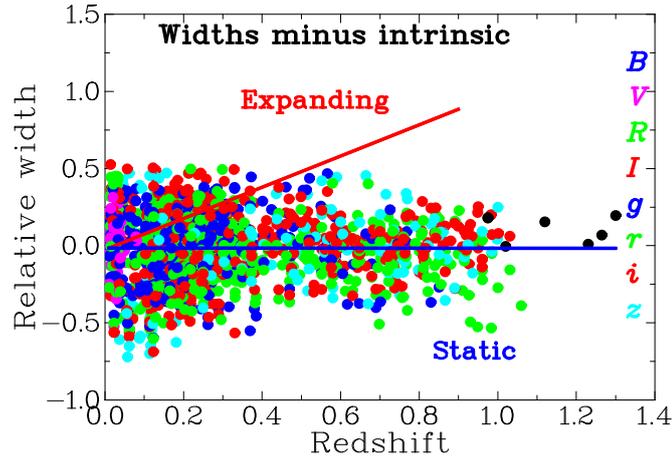

Figure 3: Relative light curve widths (without any corrections for time dilation) from the original observations for each filter minus the intrinsic width. The blue line is the regression equation $w = -0.017 - 0.001z$. The red line is what would be expected if the supernovae had time dilation of $(1 + z)$.

6.1. Apparent extra wide SNe

There are reports of SNe with very wide light curves that are inconsistent with a static model. An example of apparent extra wide light curves is the 14 light curves shown by Suzuki et al. [32]. For these supernovae the redshifts vary from 0.623 to 1.415 and the light curve (expansion model) widths vary from 1.48 to 2.43. These SNe were analyzed using SALT2 method where the static model widths are equal to the stretch factors. Thus the relative static widths vary from 0.77 to 1.09 which are well within the expected range. In a static universe the multiplication of the stretch factors by $(1 + z)$ to get the widths is unwarranted.

7. Type Ia supernovae magnitudes

The analysis for magnitudes is more complicated than that for widths in that a static model distance modulus must be used so that absolute magnitudes can be compared between the two models. Because it shows excellent results from quasar observation the curvature cosmology, briefly described in Appendix A, is used here. In order to determine the set of reference templates from SNe at all redshifts the observed apparent magnitudes must be converted to absolute magnitudes and observed wavelengths must be converted to rest-frame wavelengths. The generation of these templates has the effect of including any systematic error in the distance modulus into the templates so that the reference light curve for any supernova can approximately match the average light curve.

The SALT2 set of templates (*Salt2_template_0.dat*) show a very strong dependence of the peak flux density for each light curve on rest-frame wavelength. Fig 4 shows a plot of this peak flux density converted to magnitudes that was derived from the reference light curves as a function of rest-frame wavelength, λ. The peak flux density was measured from the average of three adjacent light curves at every second wavelength (i.e. at a step of 1 nm). The light curve flux densities were converted to magnitudes and the peak magnitudes were estimated using the parabolic procedure described in section 5. The red curve shows the intrinsic magnitude for the original observations using an expansion model and the blue line shows the intrinsic magnitude for a static model (section 5).

The differences between the peak magnitudes as a function of rest-frame wavelength is very obvious and it shows how important the choice of distance modulus can be in measuring the intrinsic peak magnitude.

A simple method of assessing which distance modulus is appropriate is to plot the observed peak absolute magnitude of SNe as a function of redshift. If the distance modulus is correct the points should scatter about a horizontal straight line. The result of the analysis in section 5 was 1568 peak magnitudes which are shown in Fig 5 both for an expanding model and for a static model.

The intrinsic magnitude correction was estimated from the intrinsic flux density distribution using filter gains. Then it was subtracted from the absolute peak flux density for each filter and for each supernova and then converted to magnitudes. The
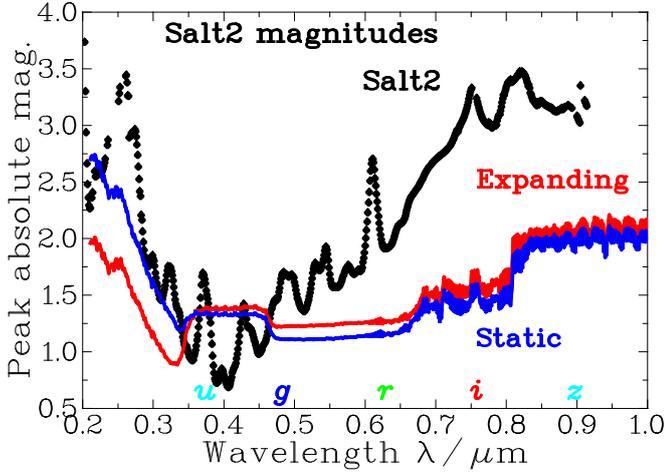
Figure 4: The black circles are a plot of the peak magnitude of the template light curves from the file, *Salt2_template_0.dat* as a function of rest-frame wavelength. The red and blue lines show the intrinsic peak magnitude distributions for an expanding model and for a static model determined from the original observations. Vertical positions are arbitrary.
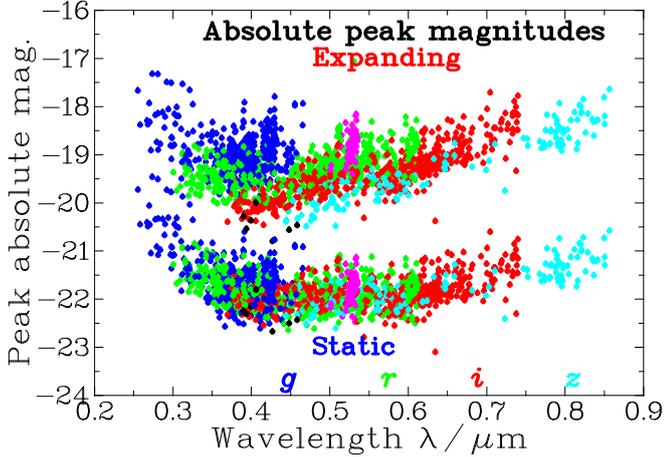

Figure 5: Observed peak absolute magnitude of type Ia supernovae as a function of rest-frame wavelength. The filters *griz* are color coded as blue, green, orange, and red respectively. The filters *BVRI* are color coded as green, magenta, orange and red respectively. The filter names are shown at their peak rest-frame wavelength. Magnitudes for all other filters are shown in black. The top set is for an expanding model and the bottom set is for a static model (offset by 3 mag).
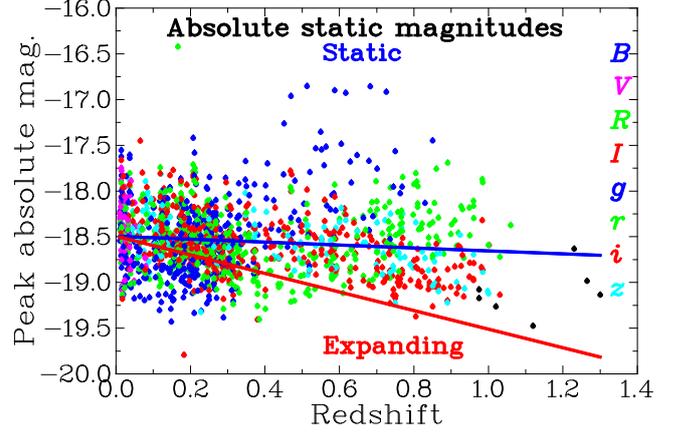

Figure 6: The colored filled circles show the peak absolute magnitudes using a static model of type Ia supernovae as shown Fig 5 but calibrated for the intrinsic magnitude distribution as a function of redshift. The blue lines shows the regression equation for a static model and the red line for an expanding model. The color code is shown vertically on the right.

Table 3: **Absolute magnitudes of peak SNe observations verses redshift,** z

model	regression	residual
expanding	$-18.682 \pm 0.010 - (1.016 \pm 0.041)z$	0.172
static	$-18.496 \pm 0.009 - (0.160 \pm 0.035)z$	0.130

result was two sets of absolute magnitudes with one set consistently analyzed using the expansion distance modulus and the second set consistently analyzed using the static distance modulus.

Table 3 shows the regression equations for each set of points and the residual rms (mag) from the regression line. Fig 6 shows a scatter diagram for the static model peak absolute magnitudes. The blue line shows the regression equation for the static model and the red line shows the regression equation for the expanding model.

The slope of the distribution of the corrected magnitude for the static model is statistically equivalent to zero which satisfies the cosmological assessment stated earlier. Clearly the scatter of points and the regression slope favor the static model as being closest to a horizontal line. Thus there is support for the hypothesis of a static universe. Note that the equation for the static distance modulus (first given Crawford [11]) has no free parameters and it has not been adjusted in any way to suit SNe observations.

It might be argued that it is not surprising that the difference between a function and its average value is constant. But in this case averaging is done at rest-frame wavelengths and the total wavelength range is only about twice the wavelength range of the filters in each supernova. If this averaging was effective then this argument would apply to both models but it is clear that the expansion model is significantly different from a constant peak magnitude.

The reason why the B14 results shown in section 4 appear

to be consistent with a constant absolute magnitude is that there is a systematic variation of the peak flux density of the light curves in the standard set of templates as a function of rest-frame wavelength. Thus we see if the B14 results (section 4) be explained in a static universe without time dilation corrections by examining the original observations. If the original absolute peak magnitudes for the expanding model are adjusted for the Salt2 magnitude correction their slope verses redshift has a coefficient -0.389 ± 0.059. If the color correction (section 4) is added it is -0.161 ± 0.057 which is statistically zero. Thus an explanation is feasible.

Although the slope for the static model could be marginally significant there is no doubt that the static model has much better agreement than the expanding model with the concept that the absolute magnitudes are independent of redshift.

7.1. Photometric redshift

The redshift of a supernovae can be estimated by comparing its wavelength spectrum to the average rest-frame wavelength spectrum as distinct from spectral wavelength measurements used to determine redshift. For example ever since Tripp [33] showed that there was a correlation between redshifts of SNe and their color index B-V there has been a considerable effort [24, 2, 21, 27, 34] to use this correlation in order to develop a predictor of the redshift from photometric measurements. However in a static universe although this is a valid estimate of the light-curve widths it is not evidence for time dilation. It is only in the expansion model that the time dilation is related to redshift.

7.2. Spectroscopic ages

Another example is spectroscopic ages. SNe show a consistent variation in characteristics of their spectra with the number of days before and after the maximum. This variation is due to changes in composition, changes in the velocity of the ejecta and the depth of penetration of the ejecta. Blondin et al. [4] have made a comprehensive analysis of these spectra for both local SNe and 13 high redshift SNe that shows that the age (the position in the light curve from the position of the peak luminosity) of a spectrum can be estimated to within 1-3 days. If there are two or more spectra the aging rate and therefore the width can be estimated. In their analysis they explicitly assumed that this width dependence was a measure of redshift which is true only for the expansion model.

8. Discussion

The normal Hubble variation of observed wavelength with redshift is well established and in an expanding universe time dilation should show the identical dependence. Observations of type Ia supernovae are one of the few observations that can directly show time dilation. However this paper shows that observations of the light curve widths type Ia supernovae do not show the effects of time dilation. The major results from this paper that support a static universe are:

- The stretch factors from a Salt2 (or similar) analysis are estimates of the intrinsic widths of supernova light curves for both expanding and static cosmologies.

- The Salt2 templates have an anomaly in their light curve widths that is in full agreement with a static universe.

- The widths of the light curves from the original observations have no redshift dependence.

- The photometric redshift relation and spectroscopic ages are consistent with a static universe.

- The apparent occurrence extra wide SNe are a consequence of using an unwarranted factor of $(1 + z)$.

- The absolute peak magnitudes of the original observations are in agreement with a static model and disagree with the standard expanding model.

8.1. Conclusions

The most important conclusions for this paper are:

- Type Ia supernovae do not show time dilations.

- The peak magnitudes of type Ia supernovae are consistent with a static universe.

- There is no dark energy in a static universe.

An important conclusion from previous Curvature Cosmology investigations (Appendix A) that is relevant here is

- Dark matter is not required in a static universe.

9. Acknowledgements

Appendix A. Static Cosmology

The static cosmology used here is Curvature Cosmology [7, 6, 8, 9, 10, 11, 12, 13, 14, 15] that is a complete cosmology that shows excellent agreement with all major cosmological observations without needing dark matter or dark energy. (Note that [15] is an update with corrections of the previous work.) It is compatible with both (slightly modified) general relativity and quantum mechanics and obeys the perfect cosmological principle that the universe is statistically the same at all places and times. It was shown in those papers that all the major observations (except supernovae) which have been used as evidence of expansion are in fact consistent with a static model.

Curvature Cosmology is based on two major hypotheses. The first hypothesis is that the Hubble redshift is due to curvature redshift, which is due to an interaction of photons with

curved spacetime where they lose energy to other very low energy photons. Thus it is a tired-light model. The basic premise is that the local quantum field describing a photon is propagated along geodesics and is therefore subject to the focussing theorem. The angular momentum is determined by a volume integral over the quantum field and if its transverse size is changed there is a change in angular momentum which is contrary to its fixed angular momentum. The resolution of this contradiction is that the photon decays into one photon with nearly all the energy and two very low energy photons. Because of symmetry the large energy photon maintains the same trajectory as the original photon. Thus there is no angular deviation that would produce fuzzy images of distant objects. The second hypothesis is that there is a reaction pressure (curvature pressure) acting on the material causing spacetime curvature from the acceleration of high velocity particles in curved spacetime. Since the acceleration of the particles is normal to their velocity there is no change in their energy. The major effect of curvature pressure is to provide stability in the cosmological model. The basic cosmology is for a simple universal model of a uniform high temperature plasma (cosmic gas) at a constant density.

The theory has a good fit to the background X-ray radiation between the energies of 10–300 keV. The fitted temperature was $2.62 \pm 0.04 \times 10^9$ K and the fitted density was equivalent to $N = 1.55 \pm 0.01$ hydrogen atoms per cubic meter (2.57×10^{-27} kg m^{-3}). For the simple homogeneous model this density is the only free parameter in the theory of curvature cosmology. The observations recorded in the cited references show that curvature cosmology is consistent with the observations of: Tolman surface brightness, angular size, gamma ray bursts, galaxy luminosity distributions, quasar luminosity distributions, X-ray background radiation, cosmic microwave background radiation, quasar variability, radio source counts, and the Butcher–Oemler effect.

In curvature cosmology the cosmic background radiation (CMB) is produced by the interaction of high energy electrons in the cosmic plasma with curved spacetime. The predicted temperature of the CMB is 3.18K to be compared with an observed value of 2.725K. The prediction does depend on the nuclei mix in the cosmic gas and could vary from this value by several tenths of a degree. It is argued that its black body spectrum arises from the large number of curvature redshift interactions undergone by the CMB photons.

In curvature cosmology the effect of a nearby high density low temperature (compared to 2.62×10^9 K) cloud is to increase the energy loss of the CMB due to curvature redshift without contributing new photons. For the Coma cluster the velocity dispersion of about 500 kms^{-1} will produce a fractional decrease of about 0.004 in the CMB temperature. The contribution from many such clouds may explain some of the CMB power spectrum.

As discussed in [14] the quasar luminosity function is close to a power law in luminosity which is equivalent to an exponential distribution in magnitude. Consequently it is possible to estimate the two constants of the luminosity function for a group of quasars that have almost the same redshift. An estimate of the average apparent peak magnitude can be derived
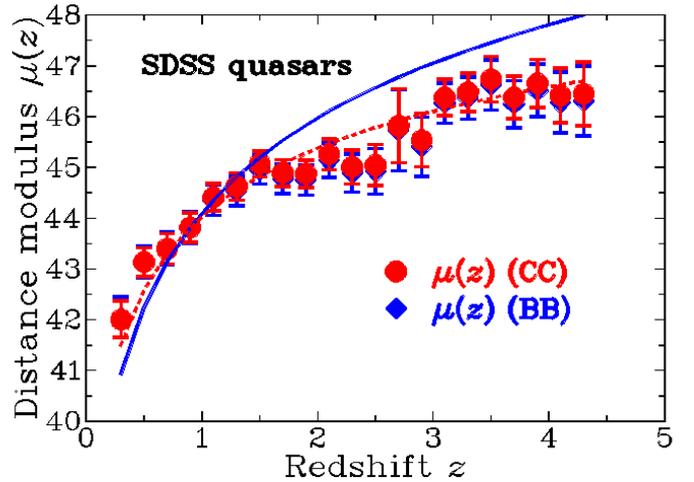

Figure A.7: Plot of the distance modulus for SDSS quasars as a function of redshift, z. The solid (blue) line and blue triangles are for concordance cosmology. The dashed (red) line and red circles are for Curvature Cosmology. This figure is taken from [14](Figure 4). The difference between the blue and red data points is due to differential volume effects. Both theoretical curves were normalized to be equal to the data point at z=0.9. Clearly Curvature Cosmology provides a better fit to the observations.

from these constants and it can be used as a "standard candle". Assuming that luminosity function is the same at all redshifts these results can be used to estimate the distance modulus. The result is shown in Fig A.7. Clearly Curvature Cosmology provides a good fit to the observations whereas the concordance results require inclusion of an evolutionary function.

Curvature redshift can explain the velocity dispersion of galaxies in the Coma cluster without requiring dark energy. Finally the anomalous acceleration of Pioneer 10 is explained by the effects of curvature redshift due to inter-planetary dust producing a very small decrease in the radio frequencies sent to and from the spacecraft.

An important result of curvature redshift is that the rate of energy loss by a photon (to extremely low energy secondary photons) as a function of distance, ds, is given by

$$\frac{1}{E}\frac{dE}{ds} = -\left(\frac{8\pi G N M_H}{c^2}\right)^{\frac{1}{2}}, \tag{A.1}$$

where M_H is the mass of a hydrogen atom and the density in hydrogen atoms per cubic metrae is $N = \rho/M_H$. Equation (A.1) shows that the energy loss is proportional to the integral of the square root of the density along the photon's path. The Hubble constant is predicted to be

$$
\begin{aligned}
H &= -\frac{c}{E}\frac{dE}{ds} = (8\pi G M_H N)^{\frac{1}{2}} \\
&= 51.69 N^{\frac{1}{2}} \, kms^{-1} \, Mpc^{-1} \tag{A.2} \\
&= 64.4 \pm 0.2 \, kms^{-1} \, Mpc^{-1} \, (N = 1.55 \pm 0.01 \, m^{-3}).
\end{aligned}
$$

The geometry is that of a three dimensional surface of a four dimensional hyper sphere. For this geometry the area of a three dimensional sphere with radius, $r = R\chi$ where $\chi = \ln(1 + z)/\sqrt{3}$ (work prior to 2009 has $\chi = \ln(1+z)/\sqrt{2}$), is given by

$$A(r) = 4\pi R^2 \sin^2(\chi). \tag{A.3}$$

The surface is finite and χ can vary from 0 to π. The total volume v, is given by

$$
\begin{aligned}
v_{static}(r) &= 2\pi R^3 \left[\chi - \frac{1}{2}\sin(2\chi) \right] \approx \frac{4\pi}{3}(R\chi)^3 \\
&= \frac{32.648}{h^3} \left[\chi - \frac{1}{2}\sin(2\chi) \right] kpc^3. \quad \text{(A.4)}
\end{aligned}
$$

The only other result required here is the equation for the distance-modulus, ($\mu_C = m - M$), which is

$$
\mu_{static} = 5 \log \left[\frac{\sqrt{3}\sin(\chi)}{h} \right] + 2.5 \log(1+z) + 42.384 \text{(A.5)}
$$

where $h = H/100\, km s^{-1}\, Mpc^{-1}$.

Appendix B. Expansion model functions

The equations needed for the modified Λ-CDM model [22, 19, 1], with $\Omega_M = 0.27$, $\Omega_K = 0$ and where h is the reduced Hubble constant, are listed below. The symbol w^* is used for the acceleration parameter in order to avoid confusion with the width, w. These equations depend on the function $E(z)$ defined here by

$$
E(z) = \int_0^z \frac{dz}{\sqrt{\Omega_M(1+z)^3 + (1-\Omega_M)(1+z)^{(1+w^*)}}}. \text{(B.1)}
$$

The distance modulus is

$$
\mu_{exp}(z) = 5 \log(E(z)(1+z)/h) + 42.384. \quad \text{(B.2)}
$$

The co-moving volume is

$$
v_{exp}(z) = \frac{4\pi}{3}(2.998 E(z)/h)^3 Gpc^3. \quad \text{(B.3)}
$$

The equation of state parameter w^* in the expansion model distance modulus is included to investigate the effects of including the cosmological constant. Conley et al. [5] found that the parameter, w^*, has a value $w^* = -0.91$, whereas Sullivan et al. [31] found that $w^* = -1.069$. Although its actual value is not critical for this paper the value of w^* is chosen to be $w^* = -1.11$.

[1] Barboza, E. M., & Alcaniz, J. S. 2008, Physics Letters B, 666, 415
[2] Bazin, G., Ruhlmann-Kleider, V., Palanque-Delabrouille, N., et al. 2011, A&A, 534, A43
[3] Betoule, M., Kessler, R., Guy, J., et al. 2014, A&A, 568, A22
[4] Blondin, S., Davis, T. M., Krisciunas, K., et al. 2008, ApJ, 682, 724
[5] Conley, A., Guy, J., Sullivan, M., et al. 2011, ApJS, 192, 1
[6] Crawford, D. F. 1987, Australian Journal of Physics, 40, 459
[7] —. 1987, Australian Journal of Physics, 40, 449
[8] —. 1991, ApJ, 377, 1
[9] —. 1993, ApJ, 410, 488
[10] —. 1995, ApJ, 440, 466
[11] —. 1995, ApJ, 441, 488
[12] —. 1999, Australian Journal of Physics, 52, 753
[13] —. 2006, Curvature Cosmology (BrownWalker Press)
[14] —. 2009 arxiv.org/abs/0901.4169
[15] —. 2009 arxiv.org/abs/1009.0953
[16] Goldhaber, G. 1997, in NATO ASIC Proc. 486: Thermonuclear Supernovae, ed. P. Ruiz-Lapuente, R. Canal, & J. Isern, 777
[17] Goldhaber, G., Boyle, B., Bunclark, P., et al. 1996, Nuclear Physics B Proceedings Supplements, Vol. 51, 51, 123
[18] Goldhaber, G., Groom, D. E., Kim, A., et al. 2001, ApJ, 558, 359
[19] Goliath, M., Amanullah, R., Astier, P., Goobar, A., & Pain, R. 2001, A&A, 380, 6
[20] Goobar, A., & Leibundgut, B. 2011, Annual Review of Nuclear and Particle Science, 61, 251
[21] Guy, J., Astier, P., Baumont, S., et al. 2007, A&A, 466, 11
[22] Hogg, D. W. 1999, ArXiv:astro-ph/9905116
[23] Holtzman, J. A., Marriner, J., Kessler, R., et al. 2008, AJ, 136, 2306
[24] Howell, D. A., Sullivan, M., Conley, A., & Carlberg, R. 2007, ApJ, 667, L37
[25] Kessler, R., Becker, A. C., Cinabro, D., et al. 2009, ApJS, 185, 32
[26] Leibundgut, B., Schommer, R., Phillips, M., et al. 1996, ApJ, 466, L21
[27] Mohlabeng, G. M., & Ralston, J. P. 2013, ArXiv e-prints
[28] Perlmutter, S., Aldering, G., Goldhaber, G., et al. 1999, ApJ, 517, 565
[29] Phillips, M. M. 1993, ApJ, 413, L105
[30] Riess, A. G., Strolger, L.-G., Casertano, S., et al. 2007, ApJ, 659, 98
[31] Sullivan, M., Guy, J., Conley, A., et al. 2011, ApJ, 737, 102
[32] Suzuki, N., Rubin, D., Lidman, C., et al. 2012, ApJ, 746, 85
[33] Tripp, R. 1998, A&A, 331, 815
[34] Wang, S., & Wang, Y. 2013, PhysRevD, 88, 043511